Physics Letters B 680 (2009) 172–178

Contents lists available at ScienceDirect

Physics Letters B

www.elsevier.com/locate/physletb

Inverse problem for the propagation equation of cosmic-ray electrons/positrons from dark matter

Koichi Hamaguchi [a,b,*], Kouhei Nakaji [a], Eita Nakamura [a]

[a] Department of Physics, University of Tokyo, Tokyo 113-0033, Japan
[b] Institute for the Physics and Mathematics of the Universe, University of Tokyo, Chiba 277-8568, Japan

ARTICLE INFO

Article history:
Received 12 May 2009
Received in revised form 24 August 2009
Accepted 24 August 2009
Available online 28 August 2009
Editor: A. Ringwald

ABSTRACT

We discuss the possibility of solving the inverse problem for the propagation equation of the cosmic-ray electrons/positrons from decaying/annihilating dark matter, and show simple analytic formulae to reconstruct the source spectrum of the electrons/positrons from the observed flux. We also illustrate our approach by applying the obtained formula to the just released Fermi data as well as the new HESS data.

1. Introduction

The existence of dark matter (DM) is by now well established [1], yet its identity is a complete mystery; it has no explanation in the framework of the Standard Model of particle physics.

Recently, several exciting data have been reported on cosmic-ray electrons and positrons, which may be indirect signatures of decaying/annihilating DM in the present universe. The PAMELA Collaboration reported that the ratio of positron and electron fluxes increases at energies of ~ 10–100 GeV [2], which shows an excess above the expectations from the secondary production of positrons. In addition, the ATIC Collaboration reported an excess of the total electron + positron flux at energies between 300 and 800 GeV [3]. (Cf. the PPB-BETS observation [4].)

More recently, the Fermi-LAT collaboration has just released precise, high-statistics data on cosmic-ray electron + positron spectrum from 20 GeV to 1 TeV [5], and the H.E.S.S. Collaboration has also reported new data [6]. Although these two new data sets show no evidence of the peak reported by ATIC, their spectra still indicate an excess above the conventional models for the background spectrum [5], and the decaying/annihilating DM remains an interesting possibility [7].

In previous studies of DM interpretations of the cosmic-ray electrons/positrons, the analyses have been done by (i) assuming a certain source spectrum from annihilating/decaying DM, (ii) solving the propagation equation and (iii) comparing the predicted electron and positron fluxes with the observation. In this Letter, we discuss the possibility of solving its inverse problem, namely, we try to reconstruct the source spectrum from the observational data.

We show that the inverse problem can indeed be solved analytically under certain assumptions and approximations, and provide analytic formulae to reconstruct the source spectrum of the electrons/positrons from the observed flux. It is found that the reconstructed spectrum in the high energy range is almost independent of the diffusion models and whether the DM is decaying or annihilating. As an illustration, we apply the obtained formulae to the electron + positron flux above ~ 100 GeV for the just released Fermi data [5], together with the new HESS data [6]. The obtained result implies that electrons/positrons at the source have a broad spectrum ranging from $\mathcal{O}(100)$ GeV to $\mathcal{O}(1)$ TeV.

2. Propagation equation of cosmic-ray electrons and positrons and its inverse problem

Let us first summarize the procedure to calculate the electron and positron fluxes. The electron/positron number density per unit kinetic energy $f_e(E,\vec{r},t)$ evolves as [8]

$$\frac{\partial}{\partial t} f_e(E,\vec{r},t) = \nabla\cdot\left[K(E,\vec{r})\nabla f_e(E,\vec{r},t)\right] + \frac{\partial}{\partial E}\left[b(E,\vec{r}) f_e(E,\vec{r},t)\right] + Q(E,\vec{r},t), \tag{1}$$

where $K(E,\vec{r})$ is the diffusion coefficient, $b(E,\vec{r})$ is the energy loss rate, and $Q(E,\vec{r},t)$ is the source term of the electrons/positrons. The effects of convection, reacceleration, and the annihilation in the Galactic disk are neglected. We only consider the electrons and positrons from DM decay/annihilation, and we assume that the source term is time-independent and spherical;

$$Q(E,\vec{r}) = q\left(|\vec{r}|\right)\frac{dN_e(E)}{dE}, \tag{2}$$

* Corresponding author at: Department of Physics, University of Tokyo, Tokyo 113-0033, Japan.
E-mail address: hama@hep-th.phys.s.u-tokyo.ac.jp (K. Hamaguchi).

0370-2693
doi:10.1016/j.physletb.2009.08.044

where dN_e/dE is the energy spectrum of the electrons and positrons from one DM decay/annihilation, and $q(|\vec{r}|)$ is given by

$$q(|\vec{r}|) = \frac{1}{m_X \tau_X}\rho(|\vec{r}|) \quad \text{for decaying DM}, \tag{3}$$

$$q(|\vec{r}|) = \frac{\langle \sigma v\rangle}{2m_X^2}\rho(|\vec{r}|)^2 \quad \text{for annihilating DM}, \tag{4}$$

where m_X and τ_X are the mass and the lifetime of the DM, $\langle \sigma v\rangle$ is the average DM annihilation cross section, and $\rho(|\vec{r}|)$ is the DM density distribution. We adopt a diffusion model with cylindrical boundary conditions, with half-height L and a radius R, and spatially constant diffusion coefficient $K(E)$ and the energy loss rate $b(E)$ throughout the diffusion zone. The steady-state propagation equation is then

$$K(E)\nabla^2 f_e(E,\vec{r}) + \frac{\partial}{\partial E}\big[b(E) f_e(E,\vec{r})\big] + q(|\vec{r}|)\frac{dN_e(E)}{dE} = 0, \tag{5}$$

with the boundary condition $f_e(E,\vec{r}) = 0$ for $r = \sqrt{x^2+y^2} = R$, $-L \leqslant z \leqslant L$ and $0 \leqslant r \leqslant R$, $z = \pm L$. As shown in Appendix A, this equation can be solved and the electron/positron number density at the Solar System, which is located at $r = r_\odot \simeq 8.5$ kpc and $z = 0$, is given by

$$f_e(E) = f_e(E,\vec{r}_\odot) = \frac{1}{b(E)}\int_E^{E_{\max}} dE' \frac{dN_e(E')}{dE'} g\big(L(E') - L(E)\big), \tag{6}$$

where

$$g(x) = \sum_{n,m=1}^{\infty} J_0\left(j_n \frac{r_\odot}{R}\right)\sin\left(\frac{m\pi}{2}\right) q_{nm} e^{-d_{nm}x}, \tag{7}$$

$$q_{nm} = \frac{2}{J_1^2(j_n)\pi}\int_0^1 d\hat{r}\,\hat{r}\int_{-\pi}^{\pi} d\hat{z}\, J_0(j_n\hat{r})\sin\left(\frac{m}{2}(\pi-\hat{z})\right) \times q\left(\sqrt{(R\hat{r})^2 + \left(\frac{L\hat{z}}{\pi}\right)^2}\right), \tag{8}$$

$$d_{nm} = \frac{j_n^2}{R^2} + \frac{m^2\pi^2}{4L^2}, \tag{9}$$

$$L(E) = \int^E dE' \frac{K(E')}{b(E')}, \tag{10}$$

and j_n are the successive zeros of J_0. The electron/positron flux is given by $\Phi_e(E) = (c/4\pi) f_e(E)$.

Our main purpose is to solve the inverse problem, i.e., to reconstruct the source spectrum $dN_e(E)/dE$ from a given flux $(c/4\pi) f_e(E)$. As shown in Appendix B, this inverse problem can indeed be solved, and the solution is given by

$$\frac{dN_e(E)}{dE} = \frac{dL(E)}{dE}\int_{-\infty}^{\infty}\frac{dk}{2\pi} e^{-ikL(E)}\frac{\int_{-\infty}^{\infty} dw\, e^{-ikw}\tilde{A}(w)}{\int_0^{\infty} dz\, e^{-ikz} g(z)}, \tag{11}$$

where

$$A(E) = f_e(E) b(E) \tag{12}$$

and

$$\tilde{A}\big(x = -L(E)\big) = A(E), \tag{13}$$

or alternatively,

$$\frac{dN_e(E)}{dE} = -\frac{1}{g(0)}\left[\frac{dA(E)}{dE} + \frac{dL(E)}{dE} \times \int_E^{E_{\max}} dE' \frac{dA(E')}{dE'}\Gamma\big(L(E') - L(E)\big)\right], \tag{14}$$

where the function $\Gamma(x)$ is determined from $g(x)$. For actual calculations in later sections, we approximate $g(x)$ by a finite sum of its leading terms. With this approximation, $\Gamma(x)$ can be computed analytically. The oscillating integrations in the left-hand side of Eq. (11) can also be calculated analytically with the approximation. See Appendix B for details.

Several comments are in order. First of all, from Eq. (14) one can see that the source flux at an energy $E_{\rm src}$ can be reconstructed once one knows the observed flux at $E_{\rm obs} \geqslant E_{\rm src}$. This may be counterintuitive, because the solution to the propagation equation (6) tells us that the observed flux at $E = E_{\rm obs}$ is determined by the source flux at $E_{\rm src} \geqslant E_{\rm obs}$. It can be understood by considering the reconstruction of the source spectrum from the highest energy and gradually to the lower energy.

Secondly, as we will see in the explicit examples, in the high energy range the above formulae can be approximated by the first term of Eq. (14);

$$\frac{dN_e(E)}{dE} \simeq -\frac{1}{g(0)}\frac{dA(E)}{dE}. \tag{15}$$

This is because at higher energies the electrons lose their energy quickly and hence only local electrons contribute. Technically, at higher energies $g(x)$ can be approximated as $g(x) \simeq g(0)$. The approximated formula Eq. (15) is then directly obtained from Eq. (6). Note that $g(0)$ is given by the local DM density $\rho_\odot \simeq 0.30\ \text{GeV/cm}^3$;

$$g(0) = q(r = r_\odot, z = 0) = \begin{cases} \rho_\odot \dfrac{1}{m_X\tau_X} & \text{for decaying DM}, \\ \rho_\odot^2 \dfrac{\langle\sigma v\rangle}{2m_X^2} & \text{for annihilating DM}. \end{cases} \tag{16}$$

3. Examples

In this section, we show some examples using the Fermi data of the electron + positron flux [5]. The purpose of this section is to demonstrate our approach and to discuss the dependence of the reconstructed source spectrum on the background spectrum and other uncertainties arising from the diffusion model and the DM density distributions. In particular, we will see that for energies $E \gtrsim 200$ GeV, the reconstructed spectrum is well approximated by the one obtained by the simple formula Eq. (15) and the dependence on the diffusion model or the DM density distribution is small.

On the other hand, in the low-energy region ($E \lesssim 100$ GeV), the reconstructed source spectrum depends on the diffusion model as well as the detailed shape of the background spectrum, and a reliable reconstruction seems difficult with the current observational data. In addition, according to the PAMELA data [2], with an assumption that the excess is mainly from the DM decay/annihilation which generates the same amount of electrons and positrons, at least about 80% of the total flux is the background in this energy range. With these observations, we focus on the energy region $E \gtrsim 100$ GeV for the reconstruction. Fortunately, as we discussed in the previous section, such an approach is valid since the source spectrum can be reconstructed using only the propagated spectrum at higher energies.

Table 1
The diffusion model parameters consistent with the observed B/C ratio [9].

Models	R [kpc]	L [kpc]	δ	K_0 [kpc^2/Myr]
M2	20	1	0.55	0.00595
MED	20	4	0.70	0.0112
M1	20	15	0.46	0.0765

For our purpose to illustrate the dependence of the reconstructed source spectrum on the background spectrum and other uncertainties, we fit the observed data by a simple polynomial function. The choice of a fitting function may seem artificial, but here it is chosen since it is convenient for applying the formulae Eq. (11) or (14) and demonstrating examples. In the next section, we present the reconstructed spectrum which does not assume any artificial fitting functions. We also ignore errors for the reconstructed spectrum arising from the experimental errors in this section. Again, this is for simplicity of demonstration and the results in the next section include the experimental errors.

Let us now begin demonstrating examples. In the propagation equation (5), the energy loss rate is taken as $b(E) = E^2/E_0\tau_E$, with $E_0 = 1$ GeV and $\tau_E = 10^{16}$ s, and the diffusion coefficient is parameterized as $K(E) = K_0(E/E_0)^\delta$, which leads to

$$L(E) = -\frac{\tau_E K_0}{1-\delta}\left(\frac{E_0}{E}\right)^{1-\delta}. \tag{17}$$

We consider the three benchmark models from Ref. [9], M2, MED, and M1, which are summarized in Table 1. The parameters K_0 and δ are chosen so that the observed B/C ratio is reproduced.

As the astrophysical background, we take a simple power law $\Phi_e^{\rm bg} \propto E^{-\alpha}$, and vary the index as $\alpha = 3.2 \pm 0.1$ to represent the effect of the background uncertainties.[1] The normalization is determined by fitting the data for $E < 100$ GeV, assuming that the electron + positron flux is dominated by the background in this energy range. The Fermi data [5] and a fitting curve, together with three different background spectra ($\alpha = 3.1$, 3.2, and 3.3) are shown in Fig. 1. We have taken as a fitting function of the observed data a polynomial of the form $E^3\Phi_e(E) = \sum_{n=0}^{5} c_n E^n$.

In Fig. 2, the source spectra reconstructed by the analytic formula [(11) or (14)] are shown for the decaying DM, with the three background spectra and the three diffusion models. Here, we assume the isothermal DM distribution $\rho(|\vec{r}|) = \rho_\odot(r_c^2 + r_\odot^2)/(r_c^2 + |\vec{r}|^2)$ with $r_c = 3.5$ kpc. We also assume that there is no excess above the energy at which the fitting curve crosses the background. As can be seen from the figure, the reconstructed source spectrum is almost independent of the diffusion models, except for the energy range $E \lesssim 200$ GeV for the M2 model with the background index $\alpha \gtrsim 3.2$. In Fig. 2, we also show the spectra obtained by the approximated formula (15). As discussed in the previous section, the simple approximation formula (15) well reproduces the results of the full formula.

In order to see the dependence on the DM density distribution (or whether DM is decaying or annihilating), we show in Fig. 3 the case of annihilating DM compared with the decaying DM, for the MED diffusion model with the background spectrum $\alpha = 3.2$. As expected, the reconstructed spectrum is almost independent of whether the DM is decaying or annihilating. This also suggests that the reconstructed spectrum does not depend on the DM density distribution very much [cf. Eqs. (3) and (4)]. These results can be understood from the approximated formula (15), which is independent of the source distribution $q(|\vec{r}|)$.

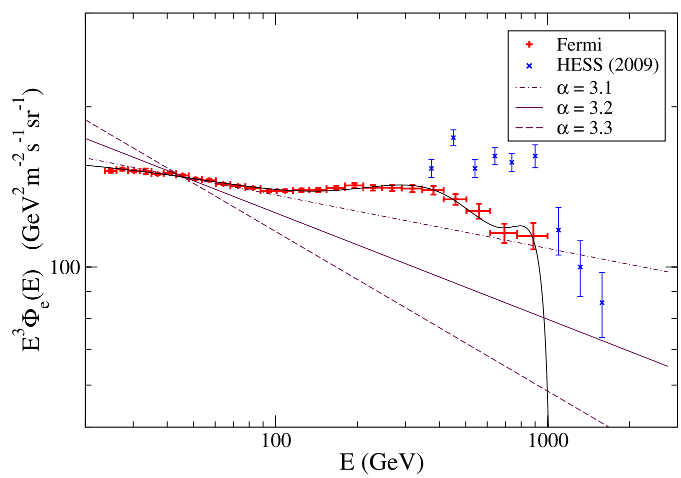

Fig. 1. The Fermi data [5] and a fitting curve, together with three different background spectra. The HESS data [6] is also shown.

4. Reconstructed source spectrum from the Fermi and HESS data

As we saw in the previous section, the reconstructed source spectrum in the high energy range $E \gtrsim 200$ GeV is almost independent of the diffusion model parameters and the DM density distribution, and the analytic formulae Eqs. (11) and (14) are well approximated by the simple formula Eq. (15).

With this result in mind, we reconstruct the source spectrum using the simple formula (15) in this section. An unsatisfactory point of the reconstruction in the previous section is that it assumes a certain fitting function. However, since the simple formula does not involve any integrals, we need not know the global spectrum of the observed flux. Therefore the reconstruction can actually be performed without choosing a global fitting function.

More precisely, the derivative $dA(E)/dE$ in Eq. (15) and the corresponding error $\delta[dA(E)/dE]$ at $E = E_i$ can be estimated by fitting a series of three data points at $E = (E_{i-1}, E_i, E_{i+1})$ with a quadratic function. Since this fitting is a local one, there is no arbitrariness in the choice of the fitting function. In this way, we can reconstruct the source spectrum directly from the experimental data.

The resultant source spectra are shown in Fig. 4 for the Fermi and HESS data. As the astrophysical background spectrum, we use the same three background spectra, with $\alpha = 3.1$, 3.2, and 3.3, as in the previous section. Here, we only adopt the statistical errors of the Fermi and HESS data [5,6]. We have also neglected the effect of finite energy resolutions. Although it is difficult to precisely reconstruct the source spectrum because of the limited data as well as the lack of the knowledge of the astrophysical background, Fig. 4 implies that the electrons/positrons from DM have a broad spectrum, ranging from $\mathcal{O}(100)$ GeV to $\mathcal{O}(1)$ TeV. For instance, a direct two-body decay of DM into electron(s), or a three-body decay into electron(s) with a smooth matrix element, would have harder spectrum and does not fit the reconstructed spectrum well. The obtained result seems to suggest that the source spectrum has a larger soft component, like the one from cascade decays.

So far, we have estimated the derivative $dA(E)/dE$ by locally fitting a series of three data points. We could as well use a series of five or more data points to estimate the derivative. As examples, the reconstructed spectra using series of five data points are shown

[1] For instance, with the parameterization in Ref. [10] based on the simulations of Ref. [11], the high energy electron + positron background spectrum is well approximated by a single power $\Phi_e^{\rm bg} = \Phi_{e^-}^{\rm bg,prim} + \Phi_{e^-}^{\rm bg,sec} + \Phi_{e^+}^{\rm bg,sec} \simeq \Phi_{e^-}^{\rm bg,prim} \propto E^{-3.25}$. The background spectrum in Ref. [12] obtained by the GALPROP code is also well approximated by a power law $\sim E^{-3.25}$ for $E \gtrsim 100$ GeV.

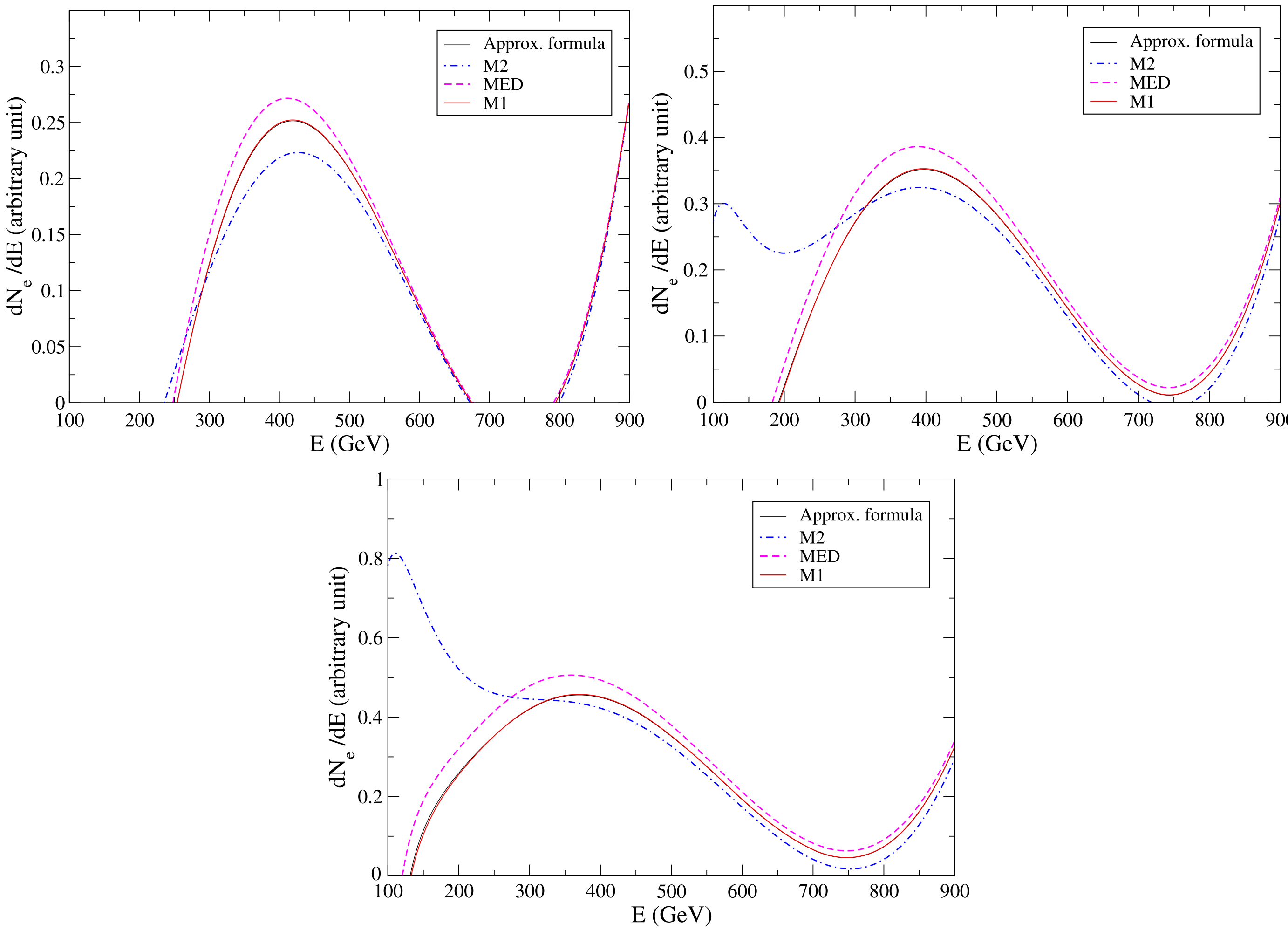

Fig. 2. The source spectra reconstructed from the Fermi data in Fig. 1, for different background spectrum indices $\alpha = 3.1$ (top left), 3.2 (top right), and 3.3 (bottom). In each case, the results of the analytic formula [(11) or (14)] are shown for the decaying DM with the three diffusion models. The spectra obtained by the simple approximation formula (15) are also shown, which almost overlap with the M1 model lines in this figure.

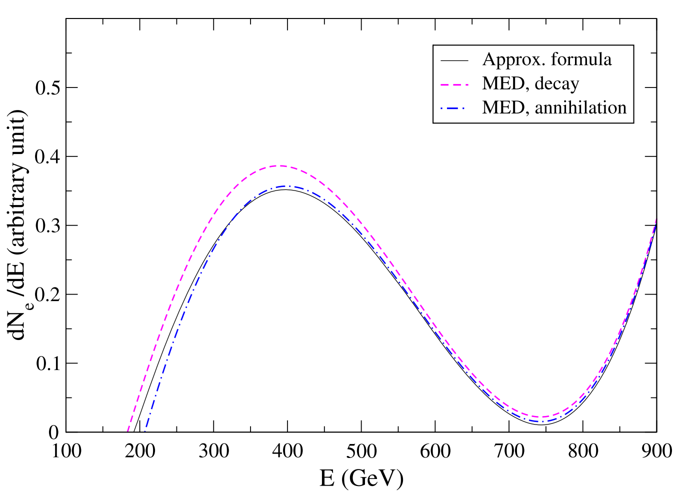

Fig. 3. The comparison of the source spectra for the decaying and annihilating DM, reconstructed from the Fermi data in Fig. 1 with a background spectrum index $\alpha = 3.2$ and the MED diffusion model. The spectrum obtained by the simple approximation formula (15) is also shown.

in Fig. 5. In the future when the data points become more dense and the errors become smaller, it will be possible to fit series of more data points to estimate the derivative for the reconstruction.

5. Discussion

In this Letter, we have discussed the possibility of solving the inverse problem for the propagation equation of the cosmic-ray electrons and positrons from the dark matter annihilation/decay. Some simple analytic formulae are shown, with which the source spectrum of the electrons and positrons can be reconstructed from the observed flux. It is shown that the reconstructed source spectrum at an energy E_{src} depends only on the observed flux above that energy, $E_{obs} \geqslant E_{src}$.

We also illustrated our approach by applying the obtained formula to the electron + positron flux above 100 GeV for the just released Fermi data [5] and the HESS data [6] assuming simple power-law backgrounds. It is shown that the reconstructed spectrum at high energy is almost independent of the diffusion models, and whether it is decaying or annihilating. Within the uncertainties, the obtained result implies that the electrons/positrons at the source have a broad spectrum ranging from $\mathcal{O}(100)$ GeV to $\mathcal{O}(1)$ TeV, with a large soft component, like the one from cascade decays.

It is difficult to precisely reconstruct the source spectrum at the present stage, because of the limited data as well as the lack of the knowledge of the astrophysical background. Future measurements, such as the PAMELA data in the higher energy range, will allow better understandings. There is also a proposed experiment CALET

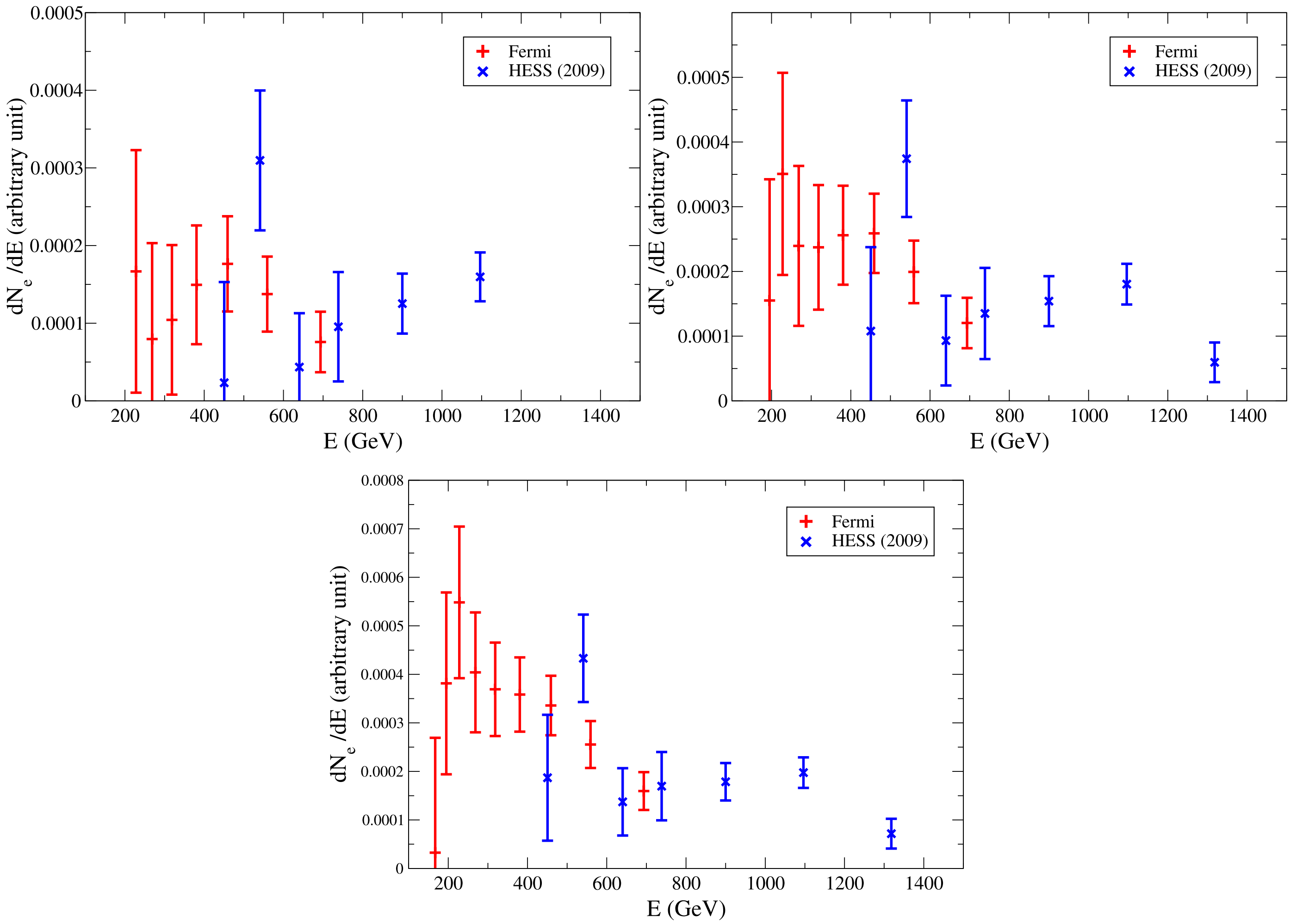

Fig. 4. The reconstructed spectrum for the Fermi and HESS data, with errors corresponding to the statistical errors of their data [5,6], with background spectrum indices $\alpha = 3.1$ (top left), 3.2 (top right), and 3.3 (bottom). See text for details.

[13], which can measure the electron + positron flux up to 10 TeV with a significant statistics (cf. [15]). We expect that our approach will be a useful tool in shedding light on the mystery of DM.

Acknowledgements

We thank Satoshi Shirai and Tsutomu Yanagida for helpful discussions and comments. This work was supported by World Premier International Center Initiative (WPI Program), MEXT, Japan. The work of E.N. is supported in part by JSPS Research Fellowships for Young Scientists.

Appendix A. Solution to the propagation equation

The propagation equation (5) can be solved in the following way (cf. Ref. [14]). Using the cylindrical coordinate, $f_e(E, \vec{r}) = f_e(E, r, z)$, where $r = \sqrt{x^2 + y^2}$ and

$$\nabla^2 = \frac{\partial^2}{\partial r^2} + \frac{1}{r}\frac{\partial}{\partial r} + \frac{\partial^2}{\partial z^2}, \tag{18}$$

the propagation equation (5) becomes

$$K(E)\left[\frac{\partial^2}{\partial r^2} + \frac{1}{r}\frac{\partial}{\partial r} + \frac{\partial^2}{\partial z^2}\right] f_e(E, r, z) + \frac{\partial}{\partial E}\big[b(E) f_e(E, r, z)\big] + q(r, z)\frac{dN_e(E)}{dE} = 0. \tag{19}$$

We expand f_e as

$$f_e(E, r, z) = \sum_{n,m=1}^{\infty} f_{nm}(E) J_0\left(j_n \frac{r}{R}\right) \sin\left(\frac{m\pi}{2L}(L - z)\right), \tag{20}$$

$$f_{nm}(E) = \frac{2}{J_1^2(j_n)\pi} \int_0^1 d\hat{r}\,\hat{r} \int_{-\pi}^{\pi} d\hat{z}\, J_0(j_n \hat{r}) \times \sin\left(\frac{m}{2}(\pi - \hat{z})\right) f_e\left(E, R\hat{r}, \frac{L}{\pi}\hat{z}\right), \tag{21}$$

where J_0 and J_1 are the zeroth and first order Bessel functions of the first kind, respectively, and j_n are the successive zeros of J_0. In this expansion, the boundary condition $f_e(E, r, z) = 0$ for $r = R$ and $z = \pm L$ is automatically satisfied. Conversely, any (sufficiently good) function which satisfies the boundary condition can be expanded as above. The orthogonal relations are

$$\int_0^1 dx\, x J_0(j_n x) J_0(j_{n'} x) = \frac{1}{2} J_1^2(j_n)\delta_{nn'}, \tag{22}$$

$$\int_{-\pi}^{\pi} dx \sin\left(\frac{m}{2}(\pi - x)\right) \sin\left(\frac{m'}{2}(\pi - x)\right) = \pi\,\delta_{mm'}$$

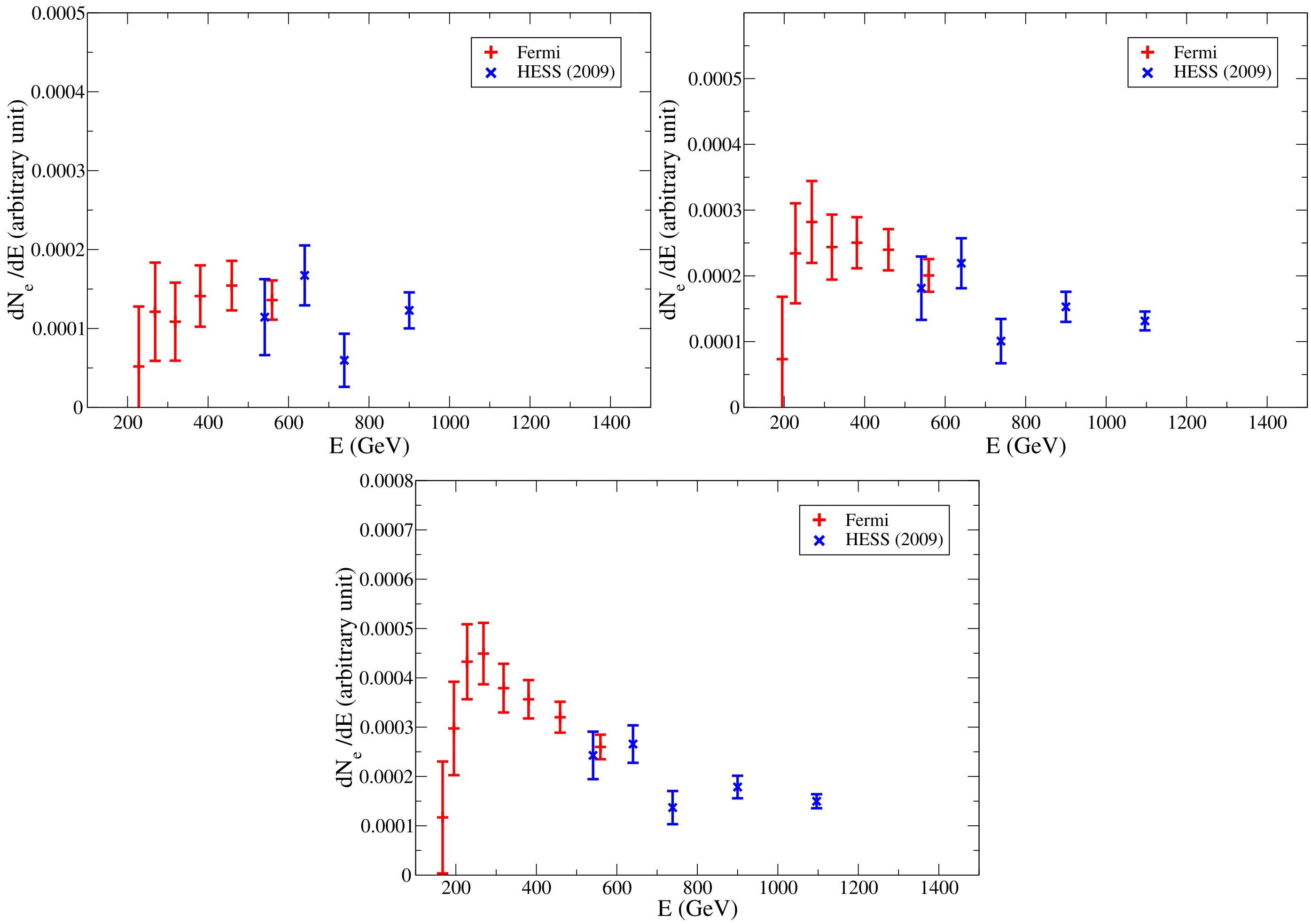

Fig. 5. The same as Fig. 4 but with series of five data points.

$$(m, m' \in \mathbb{Z}_{>0}). \tag{23}$$

Using the differential equation

$$\left[\frac{d^2}{dx^2} + \frac{1}{x}\frac{d}{dx} + j_n^2\right] J_0(j_n x) = 0, \tag{24}$$

one obtains

$$\left[-d_{nm} K(E) + \frac{\partial b(E)}{\partial E} + b(E)\frac{\partial}{\partial E}\right] f_{nm}(E) + q_{nm}\frac{dN_e(E)}{dE} = 0, \tag{25}$$

where d_{nm} and q_{nm} are given by Eqs. (9) and (8). Imposing the boundary condition for $f_{nm}(E)$ as

$$f_{nm}(E_{\max}) = 0, \quad \text{where } E_{\max} = \max\{E \mid Q_{nm}(E) \neq 0\}, \tag{26}$$

the solution to Eq. (25) is given by

$$f_{nm}(E) = \frac{1}{b(E)} \int_E^{E_{\max}} dE' \frac{dN_e(E')}{dE'} q_{nm} \times \exp\left[-d_{nm}\left(L(E') - L(E)\right)\right], \tag{27}$$

where $L(E)$ is given by Eq. (10). This leads to Eq. (6).

Appendix B. Solution to the inverse problem

Here we show two ways of reconstructing the source spectrum $dN_e(E)/dE$.

By a change of variables, Eq. (6) is rewritten as

$$\tilde{A}(x) = -\int_0^x dy \frac{d\tilde{N}_e(y)}{dy} g(x-y), \tag{28}$$

where $x = -L(E)$, $y = -L(E')$, $\tilde{N}_e(y = -L(E')) = N_e(E')$, $A(E) = f_e(E)b(E)$, and $\tilde{A}(x = -L(E)) = A(E)$. We assumed $L(E_{\max}) = 0$. Here, $\tilde{A}(x)$ and $g(x)$ are known functions once we fix the diffusion model and have the observational data. Our inverse problem is now reduced to the problem of solving for the function $d\tilde{N}_e(x)/dx$, given the functions $\tilde{A}(x)$ and $g(x)$.

The integral equation (28) is of the form known as the Volterra's integral equation. It is known that the solution of the equation exists and is unique.

We see that the right-hand side of Eq. (28) is a convolution of two functions, so the Fourier transform or the Laplace transform seems to be useful tools. In the following, we solve the equation in two different ways using the Fourier and Laplace transforms.

B.1. Fourier transform

Inserting two step functions in the integral, we get

$$\tilde{A}(x) = -\int_{-\infty}^{\infty} dy \frac{d\tilde{N}_e(y)}{dy} \theta(y) g(x-y)\theta(x-y). \tag{29}$$

Operating $\int_{-\infty}^{\infty} dx\, e^{-ikx}$ on each side of the equation and changing the variable as $z = x - y$ in the right-hand side, we obtain

$$\int_{-\infty}^{\infty} dx\, e^{-ikx} \tilde{A}(x) = -\int_{-\infty}^{\infty} dy\, e^{-iky} \frac{d\tilde{N}_e(y)}{dy} \theta(y) \int_{-\infty}^{\infty} dz\, e^{-ikz} g(z)\theta(z). \tag{30}$$

After dividing each side by $\int_{-\infty}^{\infty} dz\, e^{-ikz} g(z)\theta(z)$ and operate $\int_{-\infty}^{\infty} \frac{dk}{2\pi} e^{ikx}$, we finally get the formula we desire as

$$\frac{d\tilde{N}_e(x)}{dx}\theta(x) = -\int_{-\infty}^{\infty} \frac{dk}{2\pi} e^{ikx} \frac{\int_{-\infty}^{\infty} dw\, e^{-ikw} \tilde{A}(w)}{\int_{-\infty}^{\infty} dz\, e^{-ikz} g(z)\theta(z)}, \tag{31}$$

or

$$\frac{dN_e(E)}{dE}\theta\big(-L(E)\big) = \frac{dL(E)}{dE} \int_{-\infty}^{\infty} \frac{dk}{2\pi} e^{-ikL(E)} \frac{\int_{-\infty}^{\infty} dw\, e^{-ikw} \tilde{A}(w)}{\int_{0}^{\infty} dz\, e^{-ikz} g(z)}. \tag{32}$$

B.2. Laplace transform

Eq. (28) can be solved in an alternative way. We first differentiate the both side of the equation with respect to x and then divide by $g(0)$. Then we obtain

$$F(x) = \varphi(x) - \int_0^x dy\, K(x-y)\varphi(y), \tag{33}$$

where

$$\varphi(x) = \frac{d\tilde{N}_e(x)}{dx}, \tag{34}$$

$$F(x) = -\frac{1}{g(0)} \frac{d\tilde{A}(x)}{dx}, \tag{35}$$

and

$$K(x) = -\frac{1}{g(0)} \frac{dg(x)}{dx}. \tag{36}$$

The Laplace transform of Eq. (33) is

$$\mathcal{L}F(\xi) = \mathcal{L}\varphi(\xi) - \mathcal{L}K(\xi)\mathcal{L}\varphi(\xi), \tag{37}$$

where we denote the Laplace transform of a function $f(x)$ by $\mathcal{L}f(\xi)$:

$$\mathcal{L}f(\xi) = \int_0^{\infty} dx\, e^{-\xi x} f(x). \tag{38}$$

This equation can be solved as

$$\varphi(x) = F(x) + \int_0^x dy\, \Gamma(x-y)F(y), \tag{39}$$

where

$$\Gamma(x) = \mathcal{L}^{-1}\left[\frac{\mathcal{L}K}{1-\mathcal{L}K}\right](x) \tag{40}$$

and $\mathcal{L}^{-1}$ denotes the inverse Laplace transform. In the original variable, the solution can be written as

$$\frac{dN_e(E)}{dE} = -\frac{1}{g(0)}\left[\frac{dA(E)}{dE} + \frac{dL(E)}{dE} \int_E^{E_{\max}} dE' \frac{dA(E')}{dE'} \times \Gamma\big(L(E') - L(E)\big)\right]. \tag{41}$$

When we approximate $g(x)$ in Eq. (7) by a finite sum of its leading terms, or equivalently, $K(x)$ by a leading finite sum as

$$K(x) = \sum_{i=1}^{I} k_i e^{-a_i x}, \tag{42}$$

with k_i and a_i being corresponding coefficients, we can calculate $\Gamma(x)$ analytically. Explicitly, $\Gamma(x)$ in this case is given as

$$\Gamma(x) = \sum_{i=1}^{I} \frac{(\lambda_i + a_1)\cdots(\lambda_i + a_I)}{(\lambda_i - \lambda_1)\cdots\widehat{(\lambda_i - \lambda_i)}\cdots(\lambda_i - \lambda_I)} e^{\lambda_i x}, \tag{43}$$

where $\lambda_1, \ldots, \lambda_I$ are the roots of the equation

$$\frac{k_1}{\lambda + a_1} + \cdots + \frac{k_I}{\lambda + a_I} - 1 = 0 \tag{44}$$

and the hat in Eq. (43) means that the corresponding factor is excluded in the product.

With the same approximation, the integrals with respect to z and k in the solution Eq. (32), which uses the Fourier transform, can also be analytically calculated, and the resulting integral is a similar one as described here.

References

[1] See, for reviews G. Bertone, D. Hooper, J. Silk, Phys. Rep. 405 (2005) 279, arXiv:hep-ph/0404175;
C. Amsler, et al., Particle Data Group, Phys. Lett. B 667 (2008) 1.
[2] O. Adriani, et al., PAMELA Collaboration, Nature 458 (2009) 607, arXiv:0810.4995 [astro-ph].
[3] J. Chang, et al., Nature 456 (2008) 362.
[4] S. Torii, et al., PPB-BETS Collaboration, arXiv:0809.0760 [astro-ph].
[5] Fermi LAT Collaboration, arXiv:0905.0025 [astro-ph.HE].
[6] F. Aharonian, et al., H.E.S.S. Collaboration, Phys. Rev. Lett. 101 (2008) 261104, arXiv:0811.3894 [astro-ph];
F. Aharonian, et al., H.E.S.S. Collaboration, arXiv:0905.0105 [astro-ph.HE].
[7] L. Bergstrom, J. Edsjo, G. Zaharijas, arXiv:0905.0333 [astro-ph.HE];
S. Shirai, F. Takahashi, T.T. Yanagida, arXiv:0905.0388 [hep-ph];
P. Meade, M. Papucci, A. Strumia, T. Volansky, arXiv:0905.0480 [hep-ph];
D. Grasso, arXiv:0905.0636 [astro-ph.HE];
C.H. Chen, C.Q. Geng, D.V. Zhuridov, arXiv:0905.0652 [hep-ph];
X.J. Bi, R. Brandenberger, P. Gondolo, T. Li, Q. Yuan, X. Zhang, arXiv:0905.1253 [hep-ph];
K. Kohri, J. McDonald, N. Sahu, arXiv:0905.1312 [hep-ph].
[8] See for example: A.W. Strong, I.V. Moskalenko, V.S. Ptuskin, Annu. Rev. Nucl. Part. Sci. 57 (2007) 285, arXiv:astro-ph/0701517.
[9] T. Delahaye, R. Lineros, F. Donato, N. Fornengo, P. Salati, Phys. Rev. D 77 (2008) 063527, arXiv:0712.2312 [astro-ph].
[10] E.A. Baltz, J. Edsjo, Phys. Rev. D 59 (1999) 023511, arXiv:astro-ph/9808243.
[11] I.V. Moskalenko, A.W. Strong, Astrophys. J. 493 (1998) 694, arXiv:astro-ph/9710124.
[12] D. Grasso, et al., FERMI-LAT Collaboration, arXiv:0905.0636 [astro-ph.HE].
[13] S. Torii, CALET Collaboration, Nucl. Phys. B (Proc. Suppl.) 150 (2006) 345;
S. Torii, J. Phys. Conf. Ser. 120 (2008) 062020.
[14] J. Hisano, S. Matsumoto, O. Saito, M. Senami, Phys. Rev. D 73 (2006) 055004, arXiv:hep-ph/0511118.
[15] C.R. Chen, K. Hamaguchi, M.M. Nojiri, F. Takahashi, S. Torii, arXiv:0812.4200 [astro-ph].